Inorg. Chem. **2007**, *46*, 5486–5498

Carboxylate Coordination Chemistry of a Mononuclear Ni(II) Center in a Hydrophobic or Hydrogen Bond Donor Secondary Environment: Relevance to Acireductone Dioxygenase

Ewa Szajna-Fuller,[†] Bonnie M. Chambers,[†] Atta M. Arif,[‡] and Lisa M. Berreau*[,†]

Department of Chemistry and Biochemistry, Utah State University, Logan, Utah 84322-0300, and Department of Chemistry, University of Utah, Salt Lake City, Utah 84112

Received July 16, 2006

A series of Ni(II) carboxylate complexes, supported by a chelate ligand having either secondary hydrophobic phenyl groups (6-Ph_2TPA, *N,N*-bis((6-phenyl-2-pyridyl)methyl)-*N*-((2-pyridyl)methyl)amine) or hydrogen bond donors (bnpapa, *N,N*-bis((6-neopentylamino-2-pyridyl)methyl)-*N*-((2-pyridyl)methyl)amine), have been prepared and characterized. X-ray crystallographic studies of [(6-Ph_2TPA)Ni($O_2C(CH_2)_2SCH_3$)]ClO_4·CH_2Cl_2 (**4·CH_2Cl_2**) and [(6-Ph_2TPA)Ni($O_2CCH_2SCH_3$)]ClO_4·1.5CH_2Cl_2 (**5·1.5CH_2Cl_2**) revealed that each complex contains a distorted octahedral Ni(II) center and a bidentate carboxylate ligand. A previously described benzoate complex ([(6-Ph_2TPA)Ni(O_2CPh)]ClO_4 (**3**)) has similar structural characteristics. Recrystallization of dry powdered samples of **3**, **4·0.5CH_2Cl_2**, and **5** from wet organic solvents yielded a second series of crystalline Ni(II) carboxylate complexes having a coordinated monodentate carboxylate ligand ([(6-Ph_2TPA)Ni(H_2O)(O_2CPh)]ClO_4 (**6**), [(6-Ph_2TPA)Ni(H_2O)($O_2C(CH_2)_2SCH_3$)]ClO_4·0.2CH_2Cl_2 (**7·0.2CH_2Cl_2**), [(6-Ph_2TPA)Ni(H_2O)($O_2CCH_2SCH_3$)]ClO_4 (**8**)) which is stabilized by a hydrogen-bonding interaction with a Ni(II)-bound water molecule. In the cationic portions of **7·0.2CH_2Cl_2** and **8**, weak CH/π interactions are also present between the methylene units of the carboxylate ligands and the phenyl appendages of the 6-Ph_2TPA ligands. A formate complex of the formulation [(6-Ph_2TPA)Ni(H_2O)(O_2CH)]ClO_4 (**9**) was isolated and characterized. The mononuclear Ni(II) carboxylate complexes [(bnpapa)Ni(O_2CPh)]ClO_4 (**10**), [(bnpapa)Ni($O_2C(CH_2)_2SCH_3$)]ClO_4 (**11**), [(bnpapa)Ni($O_2CCH_2SCH_3$)]ClO_4 (**12**), and [(bnpapa)Ni(O_2CH)]ClO_4 (**13**) were isolated and characterized. Two crystalline solvate forms of **10 (10·CH_3CN** and **10·CH_2Cl_2)** were examined by X-ray crystallography. In both, the distorted octahedral Ni(II) center is ligated by a bidentate benzoate ligand, one Ni(II)-bound oxygen atom of which accepts two hydrogen bonds from the supporting bnpapa chelate ligand. Spectroscopic studies of **10**–**13** suggest that all contain a bidentate carboxylate ligand, even after exposure to water. The combined results of this work enable the formulation of a proposed pathway for carboxylate product release from the active site Ni(II) center in acireductone dioxygenase.

Introduction

Carboxylate ligation is found for metal centers in a variety of metalloenzymes.[1] The chemical factors that influence the coordination mode of a carboxylate ligand continue to be elucidated. For example, Yoon and Lippard recently described changes in the structural and O_2 reactivity properties of diiron(II) carboxylate complexes that occur as a function of the amount of water present in the reaction mixture.[2−4]

The Ni(II)-containing enzyme acireductone dioxygenase (Ni(II)-ARD) catalyzes a reaction that is a shunt out of the methionine salvage pathway in *Klebsiella ATCC 8724*.[5−8]

* Corresponding author. E-mail: berreau@cc.usu.edu. Phone: (435) 797-1625. Fax: (435) 797-3390:
[†] Utah State University.
[‡] University of Utah.

(1) Holm, R. H.; Kennepohl, P.; Solomon, E. I. *Chem. Rev.* **1996**, *96*, 2239−2314.
(2) Yoon, S.; Lippard, S. J. *J. Am. Chem. Soc.* **2004**, *126*, 16692−16693.
(3) Yoon, S.; Kelly, A. E.; Lippard, S. J. *Polyhedron* **2004**, *23*, 2805−2812.
(4) Yoon, S.; Lippard, S. J. *J. Am. Chem. Soc.* **2005**, *127*, 8386−8397.
(5) Wray, J. W.; Abeles, R. H. *J. Biol. Chem.* **1993**, *268*, 21466−21469.
(6) Wray, J. W.; Abeles, R. H. *J. Biol. Chem.* **1995**, *270*, 3147−3153.
(7) Dai, Y.; Wensink, P. C.; Abeles, R. H. *J. Biol. Chem.* **1999**, *274*, 1193−1195.
(8) Dai, Y.; Pochapsky, T. C.; Abeles, R. H. *Biochemistry* **2001**, *40*, 6379−6387.

10.1021/ic061316w CCC: $37.00 © 2007 American Chemical Society
Published on Web 02/09/2007

Scheme 1

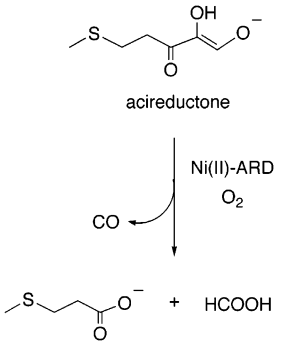

This reaction results in the production of carboxylate/carboxylic acid products via the oxidative degradation of 1,2-dihydroxy-3-keto-5-(methylthio)pentene (acireductone, Scheme 1). While the X-ray crystal structure of Ni(II)-ARD from *Klebsiella ATCC 8724* has not been reported, the ligand environment of the nickel center has been investigated by X-ray absorption spectroscopy (XAS),[9] as well as by NMR and conserved domain homology modeling methods.[10,11] The resting state mononuclear Ni(II) center exhibits pseudo-octahedral coordination, with 6 O/N donors, of which 3−4 are histidine residues. Conserved domain homology modeling of the active site in resting state Ni(II)-ARD, via comparison with jack bean canavalin, is consistent with three histidine ligands and one glutamate donor to the nickel center.[10] For the enzyme−substrate complex, XAS studies suggest that the Ni(II) center is also pseudo-octahedral, with the best fit of the data being for a primary coordination environment containing two short O/N donors. These two short donors are suggested to be from bidentate coordination of a dianionic form of the acireductone substrate. Formation of the enzyme−substrate complex is suggested to involve displacement of one histidine ligand and one water molecule. These investigations, coupled with additional results from spectroscopic and mechanistic studies, enabled a proposed mechanism to be put forth for Ni(II)-ARD (Scheme 2).[9,10] Notably, there has been nothing reported to date as to how the products of the Ni(II)-ARD reaction may interact with the Ni(II) center.

NMR and conserved domain homology modeling studies have also provided insight into the secondary environment surrounding the metal center in Ni(II)-ARD.[10,11] Two phenylalanine residues (Phe92 and Phe142) have been identified as being close enough to the Ni(II) center to have paramagnetically broadened NMR resonances.[10] It has been proposed that these residues may be involved in orienting the bound substrate properly for the reaction with O_2.

We recently reported the first reactive model system for Ni(II)-containing ARD enzymes (Scheme 3).[12,13] Specifically,

Scheme 2 Proposed Mechanism for Substrate Oxidation Catalyzed by Ni(II)-ARD

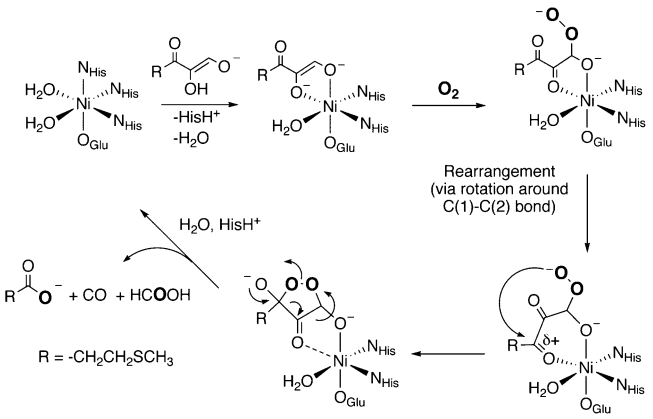

Scheme 3

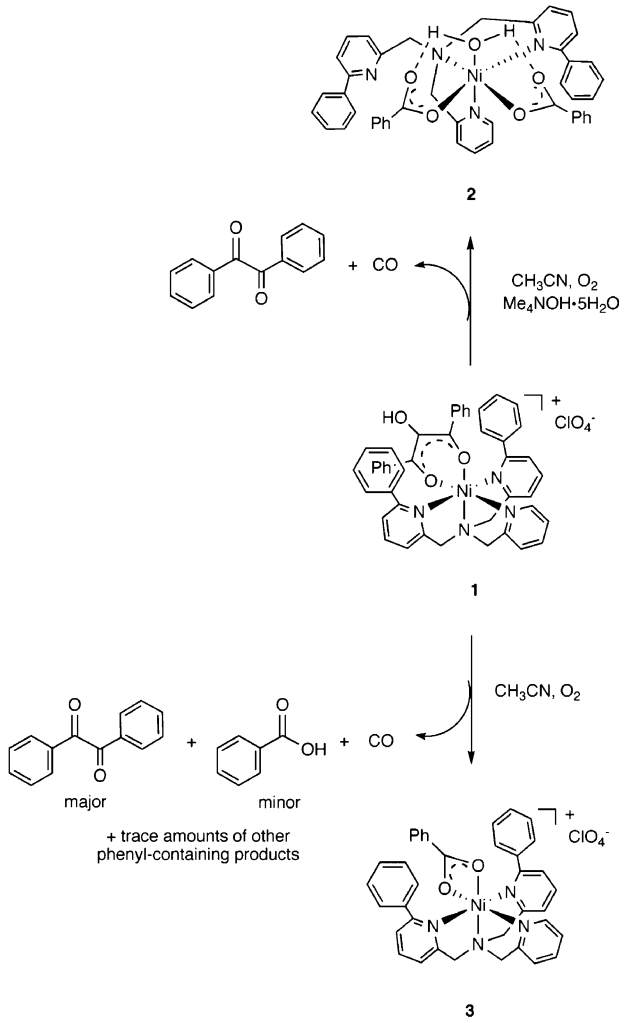

a synthetic Ni(II) complex, supported by the 6-Ph_2TPA ligand, and having a coordinated *cis*-β-keto-enolate ligand (**1**), has been shown to undergo reaction with O_2 under conditions wherein the bound enolate is in either a dianionic or monoanionic form.[12,13] These reactions result, in part, in the formation of Ni(II) carboxylate complexes (**2** and **3**) and CO as products. As shown in Scheme 3, these complexes exhibit differing coordination motifs for the 6-Ph_2TPA ligand

(9) Al-Mjeni, F.; Ju, T.; Pochapsky, T. C.; Maroney, M. J. *Biochemistry* **2002**, *41*, 6761−6769.
(10) Pochapsky, T. C.; Pochapsky, S. S.; Ju, T.; Mo, H.; Al-Mjeni, F.; Maroney, M. J. *Nat. Struct. Biol.* **2002**, *9*, 966−972.
(11) Pochapsky, T. C.; Pochapsky, S. S.; Ju, T.; Hoefler, C.; Liang, J. *J. Biomol. NMR* **2006**, *34*, 117−127.
(12) Szajna, E.; Arif, A. M.; Berreau, L. M. *J. Am. Chem. Soc.* **2005**, *127*, 17186−17187.
(13) Szajna-Fuller, E.; Rudzka, K.; Arif, A. M.; Berreau, L. M. *Inorg. Chem.* **2007**, *46*, 1471−1480.

(κ^4 versus κ^3) and monodentate versus bidentate carboxylate coordination.

In the work described herein, we have further examined the carboxylate coordination chemistry of the 6-Ph_2TPA-supported Ni(II) center. Efforts to independently synthesize the bisbenzoate derivative **2** were not successful, with the monobenzoate complex **3** instead being produced. This indicates that the formation of **2** requires more than just mixing of the individual components. In further examining the coordination chemistry of monocarboxylate derivatives (e.g., **3**, Scheme 3), we have found that, within the hydrophobic secondary environment produced by the 6-Ph_2-TPA ligand, the carboxylate ligand coordinates differently depending on the water content of the reaction mixture. Under relatively water-free conditions, the carboxylate ligand is bidentate, as is found in **3** (Scheme 3). However, when sufficient water is present, the carboxylate ligand is monodentate and forms a hydrogen-bonding interaction with a Ni(II)-bound water molecule. This water-dependent bidentate versus monodentate coordination behavior occurs for a variety of carboxylate ligands, including 3-methylthiopropionate, which is a product generated in the reaction catalyzed by Ni(II)-ARD. Interestingly, when the phenyl groups of the 6-Ph_2TPA ligand are replaced by hydrogen-bond donor secondary amine appendages in the bnpapa chelate ligand, only bidentate carboxylate coordination has been identified, even in the presence of water. These results demonstrate that the secondary environment surrounding a mononuclear Ni(II) center influences the coordination properties of a carboxylate ligand. In terms of Ni(II)-ARD, the results presented herein enable the formulation of a proposed pathway for carboxylate product release in the active site of Ni(II)-ARD.

Experimental Section

General. All reagents were obtained from commercial suppliers and were used as received unless otherwise noted. Solvents for water-sensitive reactions were dried according to published procedures and were distilled under N_2 prior to use.[14] Water-sensitive reactions were performed in an MBraun Unilab glovebox under an atmosphere of purified N_2. The 6-Ph_2TPA (*N*,*N*-bis((6-phenyl-2-pyridyl)methyl)-*N*-((2-pyridyl)methyl)amine) ligand was synthesized following a literature procedure.[15] The benzoate complex [(6-Ph_2TPA)Ni(O_2CPh)]ClO_4 (**3**) was prepared as previously described.[13]

Physical Methods. ^{1}H and ^{2}H NMR spectra of paramagnetic Ni(II) complexes were collected as previously described.[16] UV−vis spectra were recorded at ambient temperature using a Hewlett-Packard 8453 diode array spectrophotometer. Infrared spectra were recorded on Shimadzu FTIR-8400 spectrometer as KBr pellets or as CH_3CN solutions. Mass spectrometry data was obtained at the Mass Spectrometry Facility, Department of Chemistry, University of California, Riverside. Atlantic Microlabs of Norcross, GA, performed elemental analyses.

Caution! *Perchlorate salts of metal complexes with organic ligands are potentially explosive. Only small amounts of material should be prepared, and these should be handled with great care.*[17]

Attempted Independent Synthesis of 2. Equimolar amounts of 6-Ph_2TPA and $Ni(ClO_4)_2\cdot 6H_2O$ were combined in CH_3CN, methanol, or CH_2Cl_2 (∼2−3 mL). Each mixture was stirred for ∼10 min. At this point, excess Na(O_2CPh) (3 equiv), dissolved in methanol/H_2O or H_2O, was added to the reaction mixture. The resulting solutions were stirred for a minimum of 12 h. For each reaction mixture, the solvent was removed under reduced pressure and a ^{1}H NMR spectrum was obtained of the remaining solid. In each case, the spectrum was consistent with the clean formation of [(6-Ph_2TPA)Ni(O_2CPh)]ClO_4 (**3**).

Treatment of [(6-Ph_2TPA)Ni(H_2O)(O_2CPh)$_2$]ClO_4 (2) with NH_4ClO_4. Formation of [(6-Ph_2TPA)Ni(O_2CPh)]ClO_4 (3). An acetonitrile slurry of **2** (11 mg, 0.13 mmol) was purged with a stream of N_2. To this solution was added dropwise a solution of NH_4ClO_4 (0.13 mmol) in CH_3CN. During this addition process, the N_2 purge was continued. After ∼1 h, the purge was stopped, and the solution was stirred overnight at ambient temperature. Removal of the solvent under reduced pressure followed by analysis of the remaining purple solid by ^{1}H NMR indicated the clean formation of [(6-Ph_2TPA)Ni(O_2CPh)]ClO_4 (**3**). Recrystallization of the solid via diethyl ether diffusion into a CH_3OH/CH_3CN solution yielded the product as purple crystals (6.5 mg, 70%).

General Method for the Preparation of 4·0.5CH_2Cl_2 and 5. A solution of $Ni(ClO_4)_2\cdot 6H_2O$ (0.10 mmol) in CH_3CN (∼2 mL) was added to a slurry of 6-Ph_2TPA (0.10 mmol) in CH_3CN (∼2 mL). The resulting mixture was stirred for 15 min at room temperature. This solution was then transferred to a vial containing $Me_4NOH\cdot 5H_2O$ (0.11 mmol). To this combined mixture was added 3-methylthiopropionic acid or methylthioacetic acid (0.11 mmol), and the resulting solution was stirred overnight at room temperature. The solvent was removed under reduced pressure. The remaining solid was dissolved in dry CH_2Cl_2 (∼5 mL), and the solution was filtered through a celite/glass wool plug. Pentane diffusion into the CH_2Cl_2 filtrate yielded **4·0.5CH_2Cl_2** or **5** as purple crystals suitable for X-ray crystallography. These crystals were crushed and dried under vacuum prior to elemental analysis.

[(6-Ph_2TPA)Ni($O_2C(CH_2)_2SCH_3$)]ClO_4·0.5CH_2Cl_2 (4·0.5CH_2Cl_2). Yield: 70%. FTIR (KBr, cm^{-1}) 1092 (ν_{ClO4}), 621 (ν_{ClO4}). Anal. Calcd for $C_{34}H_{33}N_4SO_6ClNi\cdot 0.5CH_2Cl_2$: C, 54.36; H, 4.50; N, 7.35. Found: C, 54.77; H, 4.49; N, 7.32.

[(6-Ph_2TPA)Ni($O_2CCH_2SCH_3$)]ClO_4 (5). Yield: 74%. FTIR (KBr, cm^{-1}) 1095 (ν_{ClO4}), 623 (ν_{ClO4}). Anal. Calcd for $C_{33}H_{31}N_4SO_6ClNi$: C, 56.15; H, 4.43; N, 7.94. Found: C, 56.05; H, 4.42; N, 7.95.

[(6-Ph_2TPA)Ni(H_2O)(O_2CPh)]ClO_4 (6). This compound was prepared in an identical manner to **3**. However, the final recrystallization involved *n*-pentane diffusion into a CH_2Cl_2:H_2O solution (∼3 mL/2 drops). Yield: 80%. FTIR (KBr, cm^{-1}) 3558 (br, ν_{OH}), 1095 (ν_{ClO4}), 623 (ν_{ClO4}). Anal. Calcd for $C_{37}H_{33}N_4O_7ClNi$: C, 60.07; H, 4.50; N, 7.57. Found: C, 59.64; H, 4.45; N, 7.40.

General Method for the Preparation of 7·0.2CH_2Cl_2 and 8. The aqua carboxylate complexes **7·0.2CH_2Cl_2** and **8** were prepared in an identical manner to **4·0.5CH_2Cl_2** and **5**, albeit water (∼2 drops) was added to the CH_2Cl_2 filtrate (∼3 mL) prior to the diffusion of *n*-pentane. For each complex, blue crystals suitable for X-ray crystallography were obtained. These crystals were crushed and dried under vacuum prior to elemental analysis.

(14) Armarego, W. L. F; Perrin, D. D. *Purification of Laboratory Chemicals*, 4th ed.; Butterworth-Heinemann: Boston, MA, 1996.
(15) Makowska-Grzyska, M. M.; Szajna, E.; Shipley, C.; Arif, A. M.; Mitchell, M. H.; Halfen, J. A.; Berreau, L. M. *Inorg. Chem.* **2003**, *42*, 7472−7488.
(16) Szajna, E.; Dobrowolski, P. D.; Fuller, A. L.; Berreau, L. M. *Inorg. Chem.* **2004**, *43*, 3988−3997.
(17) Wolsey, W. C. *J. Chem. Educ.* **1973**, *50*, A335−A337.

[(6-Ph$_2$TPA)Ni(H$_2$O)(O$_2$C(CH$_2$)$_2$SCH$_3$)]ClO$_4$·0.2CH$_2$Cl$_2$ (7·0.2CH$_2$Cl$_2$). Yield: 72%. FTIR (KBr, cm^{-1}) 3466 (br, ν_{OH}), 1098 (ν_{ClO4}), 623 (ν_{ClO4}). Anal. Calcd for $C_{34}H_{35}N_4SO_7ClNi\cdot0.2CH_2Cl_2$: C, 54.42; H, 4.73; N, 7.42. Found: C, 54.54; H, 4.65; N, 7.80.

[(6-Ph$_2$TPA)Ni(H$_2$O)(O$_2$CCH$_2$SCH$_3$)]ClO$_4$ (8). Yield: 65%. FTIR (KBr, cm^{-1}) 3391 (br, ν_{OH}), 1092 (ν_{ClO4}), 621 (ν_{ClO4}). Anal. Calcd for $C_{33}H_{33}N_4SO_7ClNi$: C, 54.76; H, 4.60; N, 7.74. Found: C, 54.73; H, 4.61; N, 7.76.

[(6-Ph$_2$TPA)Ni(H$_2$O)(O$_2$CH)]ClO$_4$ (9). A solution of Ni(ClO$_4$)$_2$·6H$_2$O (0.014 g; 0.038 mmol) in CH$_3$OH (~2 mL) was added into a slurry of 6-Ph$_2$TPA (0.017 g; 0.038 mmol) in 2 mL of CH$_3$OH and stirred for ~15 min. To this solution was added an excess of sodium formate (0.008 g; 0.115 mmol) in 2 mL of H$_2$O, and the resulting mixture was stirred for ~20 h. The solvent was removed under reduced pressure, and the residue was dissolved in CH$_2$Cl$_2$ and filtered though a glass wool/Celite plug. Et$_2$O diffusion into the CH$_2$Cl$_2$ filtrate yielded pale yellow crystals suitable for X-ray crystallography (0.020 g, 81%). FTIR (KBr, cm^{-1}) 3470 (br, ν_{OH}), 1096 (ν_{ClO4}), 623 (ν_{ClO4}). Anal. Calcd for $C_{31}H_{29}N_4O_7ClNi\cdot0.33CH_2Cl_2$: C, 54.38; H, 4.32; N, 8.10. Found: C, 54.30; H, 4.46; N, 8.15. Trace CH$_2$Cl$_2$ was present in the elemental analysis sample of **9**. This solvate is not present in the X-ray crystallographically characterized sample of **9**.

***N,N*-Bis((6-pivalolylamido-2-pyridyl)methyl)-*N*-((2-pyridyl)-methyl)amine (bppapa).** A synthetic procedure for this compound has been previously reported.[18] Starting from the same precursors, a slightly different synthetic procedure was performed using CH$_3$CN and Na$_2$CO$_3$ as the solvent and base, respectively.[19] The crude brown oil obtained was used in the preparation of bnpapa without further purification.

***N,N*-Bis((6-neopentylamino-2-pyridyl)methyl)-*N*-((2-pyridyl)-methyl)amine (bnpapa).** A detailed synthetic procedure for this ligand has not been previously reported. A 100 mL round-bottom flask was charged with bppapa (0.16 g, 0.36 mmol) and dry Et$_2$O (30 mL). After purging this solution with N$_2$, LiAlH$_4$ (0.17 g, 4.4 mmol) was added in small portions. The resulting solution was stirred overnight at ambient temperature. Water was then added dropwise until no further reaction was observable. The organic/aqueous mixture was then extracted with ethyl acetate (3 × 30 mL), and the combined organic fractions were dried over Na$_2$SO$_4$. Filtration, followed by removal of the solvent from the filtrate under reduced pressure, yielded the crude product as a brown oil. Purification of this oil via column chromatography on silica gel (230−400 mesh; 92% 9/1 ethyl acetate/hexanes + 8% NEt$_3$) yielded the product as a yellow oil (72%). ^{1}H NMR (CD$_3$CN, 400 MHz) δ 8.47 (m, 1H), 7.74−7.69 (m, 2H), 7.35 (t, J = 8.1 Hz, 2H), 7.19−7.17 (m, 1H), 6.76 (d, J = 7.1 Hz, 2H), 6.34 (d, J = 8.2 Hz, 2H), 5.01 (br, 2H), 3.84 (s, 2H), 3.61 (s, 4H), 3.17 (d, J = 6.3 Hz, 4H), 0.93 (s, 18H).

[(bnpapa)Ni(O$_2$CPh)]ClO$_4$ (10). This compound was prepared in an identical manner to **3**. Crystals suitable for single-crystal X-ray diffraction were obtained by storing a CH$_3$CN/Et$_2$O (~1/20) or a CH$_2$Cl$_2$/acetonitrile/water solution of the complex at ambient temperature for several days. Yield: 47% (from CH$_3$CN:Et$_2$O). FTIR (KBr, cm^{-1}) 3336 (ν_{NH}), 1093 (ν_{ClO4}), 624 (ν_{ClO4}). Anal. Calcd for $C_{35}H_{45}N_6O_6ClNi$: C, 56.81; H, 6.13; N, 11.36. Found: C, 56.42; H, 6.25; N, 11.76.

General Method for Preparation of 11 and 12. These complexes were prepared in a similar manner to **4·0.5CH$_2$Cl$_2$** and **5**. Crystalline samples of **11** and **12** were obtained by dissolving the powdered complex (derived from removal of the CH$_2$Cl$_2$ from the filtrate) in a minimal amount of CH$_3$CN (~10 mg/0.5 mL) followed by the addition of ~20 mL of Et$_2$O. Storing of these solutions at ambient temperature for ~12−24 h resulted in the deposition of purple crystals, which were crushed and dried prior to elemental analysis. In general, the yield of the bnpapa-ligated complexes is low due to their high solubility in a variety of organic solvents.

[(bnpapa)Ni(O$_2$C(CH$_2$)$_2$SCH$_3$)]ClO$_4$ (11). Yield: 46%. FTIR (KBr, cm^{-1}) 3335 (ν_{NH}), 1090 (ν_{ClO4}), 621 (ν_{ClO4}). Anal. Calcd for $C_{32}H_{47}N_6SO_6ClNi$: C, 52.08; H, 6.42; N, 11.39. Found: C, 52.43; H, 6.50; N, 11.41.

[(bnpapa)Ni(O$_2$CCH$_2$SCH$_3$)]ClO$_4$ (12). Yield: 63%. FTIR (KBr, cm^{-1}) ~3300 (br, ν_{NH}), 1082 (ν_{ClO4}), 621 (ν_{ClO4}). Anal. Calcd for $C_{31}H_{45}N_6SO_6ClNi$: C, 51.43; H, 6.27; N, 11.61. Found: C, 51.54; H, 6.38; N, 11.63.

[(bnpapa)Ni(O$_2$CH)]ClO$_4$ (13). This complex was prepared in a similar manner to **9**, albeit water was not added to the reaction mixture. Yield: 54%. FTIR (KBr, cm^{-1}) 3340 (br, ν_{NH}), 1092 (ν_{ClO4}), 623 (ν_{ClO4}). Anal. Calcd for $C_{29}H_{41}N_6O_6ClNi$: C, 52.47; H, 6.23; N, 12.66. Found: C, 52.37; H, 6.23; N, 12.63.

***d*$_6$-bnpapa (Benzylic Deuteration).** To bnpapa (0.19 g, 4.0 × 10^{-4} mol) in a round-bottom flask was added CH$_3$C(O)OD (9 mL, Aldrich, 98%). The resulting solution was refluxed under nitrogen for 12 h. After cooling to room temperature, the reaction mixture was transferred to a 250 mL Erlenmeyer flask, and aqueous NaOH (5 M) was carefully added dropwise until the pH > 11. To this solution was added CH$_2$Cl$_2$ (40 mL), and the solution was stirred for 1.5 h at room temperature. The CH$_2$Cl$_2$ layer was then removed, and the aqueous layer was further extracted with additional CH$_2$Cl$_2$ (2 × 40 mL). The combined organic fractions were dried over sodium sulfate, the solution was filtered, and the filtrate was brought to dryness by rotary evaporation. The remaining dark brown oil was used for the synthesis of Ni(II) carboxylate complexes without further purification. ^{1}H NMR (CD$_3$CN, 300 MHz) δ 8.44 (d, J = 5.2 Hz, 1H), 7.67 (d, J = 3.8 Hz, 2H), 7.36−7.28 (m, 2H), 7.20−7.12 (m, 1H), 6.71 (d, J = 7.2 Hz, ~1H), 6.32 (d, J = 8.6 Hz, 2H), 5.03 (br s, ~2H, N−*H*), 3.13 (d, J = 6.5 Hz, 4H), 0.91 (s, 18H) ppm. Low integration of the aromatic resonance at 6.71 ppm indicates partial deuteration of a β-H position of the amine-appended pyridyl ring. Incorporation of deuterium at the benzylic position is >95% as indicated by the fact that singlets found at 3.84 and 3.61 ppm in the ^{1}H NMR of the bnpapa ligand are not observed in the ^{1}H NMR of *d*$_6$-bnpapa. ^{2}H NMR (CD$_3$CN, 46 MHz) δ 6.8, 3.8, 3.6 ppm.

***d*$_4$-bnpapa (Neopentyl Methylene Deuteration).** The amide-containing bppapa (0.32 g, 6.5 × 10^{-4} mol) was combined with LiAlD$_4$ (12 equiv) in dry diethyl ether (50 mL). This mixture was stirred for approximately 12 h at room temperature under a nitrogen atmosphere. Water (~15 mL) was carefully added dropwise until no frothing occurred. This solution was then extracted with ethyl acetate (3 × 50 mL). The combined organic fractions were dried over sodium sulfate. Following filtration, the filtrate was brought to dryness under reduced pressure which yielded a pale brown oil. Column chromatography on silica gel using the conditions outlined above for the bnpapa ligand yielded the *d*$_4$-labeled ligand a yellow oil. ^{1}H NMR (CD$_3$CN, 300 MHz) δ 8.43 (d, J = 4.8 Hz, 1H), 7.70−7.62 (m, 2H), 7.34−7.27 (m, 2H), 7.15−1.11 (m, 1H), 6.73 (d, J = 7.2 Hz, 2H), 6.30 (d, J = 8.3 Hz, 2H), 5.01 (br, 2H), 3.80 (s, 2H), 3.57 (s, 4H), 0.93 (s, 18H) ppm. ^{2}H NMR (CD$_3$CN, 46 MHz) δ 3.14 ppm.

(18) Harata, M.; Hasegawa, K.; Jitsukawa, K.; Masuda, H.; Einaga, H. *Bull. Chem. Soc. Jpn.* **1998**, *71*, 1031−1038.
(19) Garner, D. K.; Fitch, S. B.; McAlexander, L. H.; Bezold. L. M.; Arif, A. M.; Berreau, L. M. *J. Am. Chem. Soc.* **2002**, *124*, 9970−9971.

[(d_6-bnpapa)Ni(O_2CPh)]ClO_4 (10-d_6), [(d_6-bnpapa)Ni(O_2C-(CH_2)$_2$$SCH_3$)]$ClO_4$ (11-d_6), and [(d_6-bnpapa)Ni(O_2CH)]ClO_4 (13-d_6) were prepared using d_6-bnpapa following identical synthetic methods as those outlined for the preparation of **10**, **11**, and **13**.

[(d_4-bnpapa)Ni(O_2CPh)]ClO_4 (10-d_4), [(d_4-bnpapa)Ni(O_2C-(CH_2)$_2$$SCH_3$)]$ClO_4$ (11-d_4), and [(d_4-bnpapa)Ni(O_2CH)]ClO_4 (13-d_4) were prepared using d_4-bnpapa following identical synthetic methods as those outlined for the preparation of **10**, **11**, and **13**.

X-ray Crystallography. Single crystals of selected compounds were mounted on a glass fiber with viscous oil and then transferred to a Nonius KappaCCD diffractometer (Mo Kα, $\lambda = 0.71073$ Å) for data collection at 150(1) K. For each compound, an initial set of cell constants was obtained from 10 frames of data that were collected with an oscillation range of 1°/frame and an exposure time of 20s/ frame. Indexing and unit cell refinement based on all observed reflections from those 10 frames indicated monoclinic *P* lattices for **4·CH_2Cl_2**, **5·1.5CH_2Cl_2**, **9**, and **10·CH_3CN**, a monoclinic *C* lattice for **7·0.5CH_2Cl_2**, triclinic *P* lattices for **6·1.75CH_2Cl_2** and **8**, and an orthorhombic *P* lattice for **10·CH_2Cl_2**. Final cell constants for each complex were determined from a set of strong reflections from the actual data collection. For each data set, these reflections were indexed, integrated, and corrected for Lorentz, polarization, and absorption effects using DENZO-SMN and SCALEPAC.[20] The structures were solved by a combination of direct methods and heavy atom using SIR97. All non-hydrogen atoms were refined with anisotropic displacement coefficients. Unless otherwise noted, hydrogen atoms were assigned isotropic displacement coefficients $U(H) = 1.2U(C)$ or $1.5U(C_{methyl})$, and their coordinates were allowed to ride on their respective carbons using SHELXL97.[21]

Structure Solution and Refinement. The methylthiopropionate complex **4·CH_2Cl_2** crystallizes in the monoclinic crystal system in the space group $P2_1/c$. All hydrogen atoms except those of a methylene chloride solvate molecule were located and refined independently. The carbon atom and one chlorine atom of this solvate molecule exhibit disorder over two positions.

Complex **5·1.5CH_2Cl_2** crystallizes in the monoclinic crystal system in the space group $P2_1/c$. All hydrogen atoms except those of the methylene chloride solvate molecules were located and refined independently. The perchlorate anion exhibits disorder, which was addressed by splitting the O(4) and O(6) atoms into two fragments (O(4)/O(4′), O(6)/O(6′)), followed by refinement. This led to a 0.88:0.12 ratio in occupancy over the two positions for each oxygen atom. The half-occupied methylene chloride is positioned near an inversion center, and the atoms of this solvate exhibit disorder.

Complex **6·1.75CH_2Cl_2** crystallizes in the triclinic crystal system in the space group $P\bar{1}$. There are two independent formula units per asymmetric unit, with the second being denoted by "A". Methylene chloride (1.75 molecules per formula unit) is present in the asymmetric unit. One methylene chloride solvate molecule is disordered.

Complex **7·0.5CH_2Cl_2** crystallizes in the monoclinic crystal system in the space group $C2/c$. All hydrogen atoms except those on C(21), C(34), and the methylene chloride solvate molecule were located and refined independently. The disordered, half-occupied molecule of methylene chloride is positioned near an inversion center.

The aqua methylthioacetate complex **8** crystallizes in the triclinic crystal system in the space group $P\bar{1}$. All hydrogen atoms except those on C(32) and C(33) were located and refined independently. The methylene carbon (C(32)), sulfur (S(1)), and methyl carbon (C(33)) atoms of the methylthioacetate ligand exhibit disorder. Each was split into two fragments (C(32)/C(32A), S(1)/S(1A), C(33)/C(33A)) followed by refinement. This resulted in a 70:30 ratio in occupancy for each atom.

Complex **9** crystallizes in the monoclinic crystal system in the space group $P2_1/n$. All hydrogen atoms were located and refined

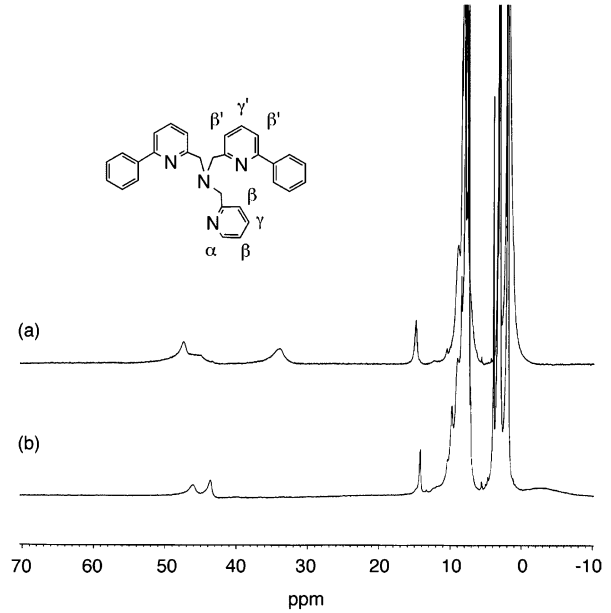

Figure 1. ^{1}H NMR spectra of (a) [(6-Ph_2TPA)Ni(O_2CPh)]ClO_4 (**3**) and (b) [(6-Ph_2TPA)Ni(H_2O)(O_2CPh)$_2$] (**2**) in CD_3CN at 25(1) °C. Inset: Labeling of proton positions for the 6-Ph_2TPA ligand.

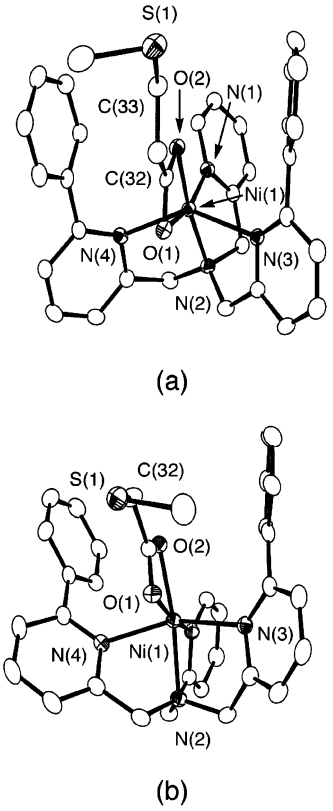

Figure 2. ORTEP representations of the cationic portions of (a) **4·CH_2Cl_2** and (b) **5·1.5CH_2Cl_2**. All ellipsoids are drawn at the 35% probability level. Hydrogen atoms have been omitted for clarity.

(20) Otwinowski, Z.; Minor, W. *Methods Enzymol.* **1997**, *276*, 307−326.
(21) Sheldrick, G. M. *SHELXL-97, Program for the Refinement of Crystal Structures*; University of Göttingen: Göttingen, Germany, 1997.

independently. Three oxygen atoms of the perchlorate anion (O(5), O(6), and O(7)) exhibit disorder. Each was split into two fragments (with the second being denoted by "A") and was refined. This refinement resulted in a 80:20 ratio in occupancy for each atom.

Complex **10·CH_3CN** crystallizes in the monoclinic crystal system in the space group $P2_1/n$ with one molecule of acetonitrile in the lattice. Complex **10·CH_2Cl_2** crystallizes in the orthorhombic crystal system in the space group $P2_12_12_1$. The secondary amine hydrogen atoms were located and refined independently in both structures.

Results

Bis- and Monobenzoate Ni(II) Complexes of the 6-Ph_2TPA Ligand. In the O_2-dependent reaction catalyzed by the Ni(II)-containing acireductone dioxygenase from *Klebsiella ATCC 8724*, carboxylate/carboxylic acid products are generated from the oxidative degradation of 1,2-dihydroxy-3-keto-5-(methylthio)pentene (acireductone, Scheme 1).[5,6] These products do not inhibit the enzyme at concentrations up to 1 mM.[8] As a means of elucidating the chemical factors that govern the O_2 reactivity and carboxylate coordination chemistry of the active site metal center in Ni(II)-ARD, we have developed a reactive synthetic model complex (**1**, Scheme 3) that exhibits single turnover Ni(II)-ARD-type reactivity.[12] This complex, which contains a coordinated *cis*-β-keto-enolate ligand as a model for the ARD substrate, undergoes reaction with O_2 under varying conditions to yield Ni(II) carboxylate complexes (**2** and **3**, Scheme 3) and CO. In the work described herein, we have further examined the coordination chemistry of the Ni(II) carboxylate products.

After identifying the bisbenzoate complex [(6-Ph_2TPA)Ni(H_2O)($O_2CPh)_2$] (**2**) as the product of the reaction of **1** and O_2 in the presence of 1 equiv of base, we attempted to independently synthesize this complex. Admixture of equimolar amounts of 6-Ph_2TPA and $Ni(ClO_4)_2$·$6H_2O$ in acetonitrile, methanol, or CH_2Cl_2 followed by the addition of excess NaO_2CPh (in methanol/H_2O or H_2O) and stirring for a minimum of 12 h at room temperature, resulted only in the isolation of [(6-Ph_2TPA)Ni(O_2CPh)]ClO_4 (**3**). Thus, **2** cannot be generated via a spontaneous self-assembly type process. We hypothesize that the reaction pathway involving **1** and O_2 in the presence of base (Scheme 3) by which **2** is formed must provide the conditions under which κ^3-coordination of the 6-Ph_2TPA ligand is accessed.

The bisbenzoate complex **2** is readily transformed into the monobenzoate derivative **3** and benzoic acid via the addition of 1 equiv of a proton donor (NH_4ClO_4, Scheme 4). This reaction is straightforward to monitor using ^{1}H NMR (Figure 1). Although both complexes exhibit broad, paramagnetically shifted resonances, the features found in the 30−50 ppm region of the spectrum are characteristic of each complex. Addition of slightly greater than 1 equiv of NH_4ClO_4 to **2** results in the formation of a mixture of **3** and [(6-Ph_2TPA)Ni($CH_3CN)_2$]($ClO_4)_2$.[15,16]

Methylthioalkyl Ni(II) Carboxylate Complexes of the 6-Ph_2TPA Ligand. An analogue of **3** having a coordinated 3-methylthiopropionate ligand, [(6-Ph_2TPA)Ni($O_2C(CH_2)_2SCH_3$)]ClO_4 (**4·0.5CH_2Cl_2**), was prepared via admixture of equimolar amounts of 6-Ph_2TPA with $Ni(ClO_4)_2$·$6H_2O$ in dry acetonitrile, followed by treatment with Me_4NOH·$5H_2O$ and 3-methylthiopropionic acid (Scheme 5). The methylthioacetate complex [(6-Ph_2TPA)Ni($O_2CCH_2SCH_3$)]ClO_4 (**5**) was prepared in a similar fashion. These complexes were characterized by X-ray crystallography, elemental analysis, ^{1}H NMR, FTIR, and FAB-MS.

Scheme 4

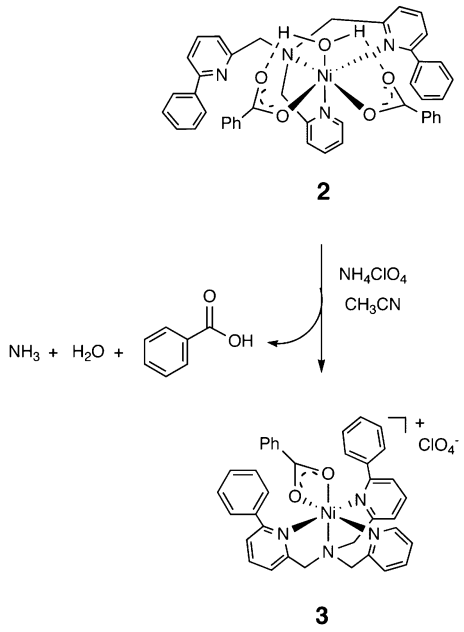

2 **3**

Scheme 5

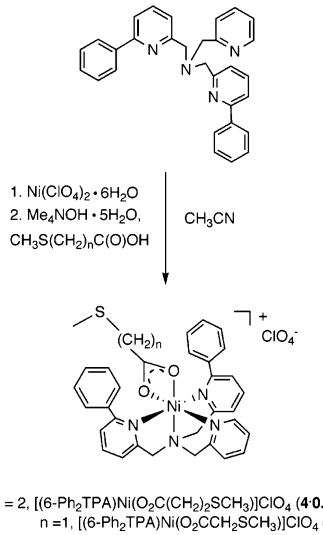

n = 2, [(6-Ph_2TPA)Ni($O_2C(CH_2)_2SCH_3$)]ClO_4 (**4·0.5CH_2Cl_2**)
n =1, [(6-Ph_2TPA)Ni($O_2CCH_2SCH_3$)]ClO_4 (**5**)

The cationic portions of the X-ray structures of **4·CH_2Cl_2** and **5·1.5CH_2Cl_2** are shown in Figure 2. Details of the X-ray data collection and refinement for these complexes are given in Table 1. Selected bond distances and angles are given in Tables 2 and 3, respectively. For comparison, included in the latter tables are bond distances and angles for [(6-Ph_2TPA)Ni(O_2CPh)]ClO_4 (**3**).

The Ni(II) carboxylate derivatives **3**, **4·CH_2Cl_2**, and **5·1.5CH_2Cl_2** each contain a mononuclear Ni(II) center ligated by a bidentate carboxylate ligand and the four available nitrogen donors of the 6-Ph_2TPA ligand. The Ni(II) center in each complex coordinates the 6-Ph_2TPA ligand with

Table 1. Summary of X-ray Data Collection and Refinement for 6-Ph_2TPA-supported Ni(II) Carboxylate Complexes

	4·CH_2Cl_2	**5·1.5CH_2Cl_2**	**6·1.75CH_2Cl_2**	**7·0.5CH_2Cl_2**	**8**	**9**
empirical formula	$C_{35}H_{35}N_4Cl_3O_6SNi$	$C_{34.5}H_{34}N_4Cl_4O_6SNi$	$C_{38.75}H_{36.5}N_4Cl_{4.5}O_7Ni$	$C_{34.5}H_{36}N_4Cl_2O_7SNi$	$C_{33}H_{33}N_4ClO_7SNi$	$C_{31}H_{29}N_4ClO_7Ni$
fw	804.79	833.23	888.45	780.34	723.85	663.74
cryst syst	monoclinic	monoclinic	triclinic	monoclinic	triclinic	monoclinic
space group	$P2_1/c$	$P2_1/c$	$P\bar{1}$	$C2/c$	$P\bar{1}$	$P2_1/n$
a (Å)	10.5995(2)	10.7355(2)	12.7841(2)	32.2278(9)	11.9609(3)	14.6776(5)
b (Å)	19.2209(7)	18.8996(4)	17.5239(4)	13.1954(4)	11.9728(3)	13.8506(6)
c (Å)	18.1175(6)	18.5336(4)	19.5938(4)	18.9364(3)	13.5445(3)	15.1681(4)
α (deg)	90	90	77.7264(12)	90	92.1279(10)	90
β (deg)	105.0839(19)	101.9763(11)	77.8212(12)	120.5857(15)	108.8245(13)	107.6192(2)
γ (deg)	90	90	70.5710(10)	90	116.0983(11)	90
V (Å^3)	3563.94(19)	3678.55(13)	3997.84(14)	6932.5(3)	1611.70(7)	2938.92(18)
Z	4	4	4	8	2	4
d_{calcd}, Mg m^{-3}	1.500	1.505	1.476	1.495	1.492	1.500
temp (K)	150(1)	150(1)	150(1)	150(1)	150(1)	150(1)
cryst size (mm^3)	0.30 × 0.20 × 0.08	0.35 × 0.25 × 0.20	0.28 × 0.25 × 0.18	0.35 × 0.25 × 0.10	0.40 × 0.35 × 0.25	0.40 × 0.25 × 0.20
diffractometer[a]	Nonius Kappa CCD	Nonius Kappa CCD	Nonius Kappa CCD	Nonius Kappa CCD	Nonius Kappa CCD	Nonius Kappa CCD
abs coeff. (mm^{-1})	0.879	0.925	0.840	0.829	0.805	0.807
2θ max (deg)	50.68	54.96	54.96	55.02	54.96	55.24
reflns collected	12031	14362	27379	13167	10742	11390
indep reflns	6489	8396	18207	7905	7268	6719
variable params	592	614	1023	578	560	526
R1/wR2[b]	0.0529/0.1245	0.0468/0.1069	0.0569/0.1378	0.0625/0.1554	0.0411/0.0949	0.0563/0.1030
GOF (F^2)	1.051	1.026	1.028	1.032	1.038	1.095
largest diff (e Å^{-3})	1.016/−0.810	1.017/−0.538	1.565/−1.070	0.985/−1.537	1.112/−0.503	0.421/−0.484

[a] Radiation used: Mo Kα (λ = 0.71073 Å). [b] $R1 = \Sigma||F_o| - |F_c||/\Sigma|F_o|$; $wR2 = [\Sigma[w(F_o^2 - F_c^2)^2]/[\Sigma(F_o^2)^2]]^{1/2}$ where $w = 1/[\sigma^2(F_o^2) + (aP)^2 + bP]$.

Table 2. Selected Bond Distances for 6-Ph_2TPA-Supported Ni(II) Carboxylate Complexes[a]

	3	**4·CH_2Cl_2**	**5·1.5CH_2Cl_2**	**6·1.75CH_2Cl_2**	**7·0.5CH_2Cl_2**	**8**	**9**
Ni(1)−N(1)	2.0282(16)	2.024(3)	2.054(2)	2.062(3)	2.072(3)	2.0537(18)	2.074(3)
Ni(1)−N(2)	2.0691(16)	2.075(3)	2.063(2)	2.089(3)	2.080(3)	2.0796(18)	2.080(3)
Ni(1)−N(3)	2.1458(16)	2.233(3)	2.198(2)	2.216(2)	2.240(3)	2.1884(17)	2.194(3)
Ni(1)−N(4)	2.2134(16)	2.193(3)	2.165(2)	2.241(2)	2.186(3)	2.2050(17)	2.218(3)
Ni(1)−O(1)	2.0521(13)	2.183(2)	2.1868(17)	2.001(2)	1.994(2)	1.9932(15)	2.001(2)
Ni(1)−O(2)	2.1293(13)	2.014(2)	2.0370(18)			2.1182(16)	
Ni(1)−O(3)				2.062(2)	2.080(3)		2.088(3)

[a] Estimated standard deviations in the last significant figure are given in parentheses.

Table 3. Selected Bond Angles for 6-Ph_2TPA-supported Ni(II) Carboxylate Complexes[a]

	3	**4·CH_2Cl_2**	**5·1.5CH_2Cl_2**	**6·1.75CH_2Cl_2**	**7·0.5CH_2Cl_2**	**8**	**9**
O(1)−Ni(1)−O(2)	63.30(5)	62.76(9)	62.37(7)			91.65(6)	
O(1)−Ni(1)−O(3)				93.76(9)	94.08(11)		93.47(10)
O(1)−Ni(1)−N(1)	108.59(6)	161.06(11)	171.30(8)	92.18(9)	91.08(11)	90.74(7)	90.26(10)
O(1)−Ni(1)−N(2)	168.33(6)	118.49(10)	107.29(8)	171.64(9)	172.47(11)	171.57(7)	171.35(10)
O(1)−Ni(1)−N(3)	94.84(6)	80.24(10)	81.53(7)	103.30(9)	99.75(11)	100.90(6)	101.12(10)
O(1)−Ni(1)−N(4)	100.81(6)	83.55(10)	81.31(7)	98.34(9)	100.72(11)	101.99(6)	99.77(10)
O(2)−Ni(1)−N(1)	170.84(6)	98.31(11)	109.09(8)			177.47(7)	
O(2)−Ni(1)−N(2)	106.49(6)	173.00(11)	168.37(8)			96.22(7)	
O(2)−Ni(1)−N(3)	83.74(5)	97.75(10)	100.32(8)			78.55(6)	
O(2)−Ni(1)−N(4)	80.59(6)	105.33(10)	94.56(8)			83.17(7)	
O(3)−Ni(1)−N(1)				172.99(10)	174.50(12)		174.46(11)
O(3)−Ni(1)−N(2)				92.19(10)	93.14(12)		94.51(11)
O(3)−Ni(1)−N(3)				93.03(9)	93.92(11)		92.21(11)
O(3)−Ni(1)−N(4)				83.59(9)	81.82(11)		81.18(10)
N(1)−Ni(1)−N(2)	81.99(7)	80.29(11)	81.36(8)	82.31(10)	81.79(12)	81.35(7)	82.02(11)
N(1)−Ni(1)−N(3)	101.75(6)	103.71(11)	99.10(8)	81.98(9)	83.28(11)	100.20(7)	83.04(10)
N(1)−Ni(1)−N(4)	97.48(6)	102.85(11)	101.78(8)	99.23(9)	99.14(11)	97.12(7)	102.23(10)
N(2)−Ni(1)−N(3)	77.80(6)	76.04(11)	82.52(8)	82.23(10)	81.87(12)	77.81(7)	81.89(11)
N(2)−Ni(1)−N(4)	82.16(6)	81.66(11)	77.93(9)	76.48(9)	78.20(12)	82.01(7)	78.21(10)
N(3)−Ni(1)−N(4)	149.83(6)	141.57(10)	148.73(8)	158.28(10)	159.33(12)	150.97(7)	158.42(11)

[a] Estimated standard deviations in the last significant figure are given in parentheses.

similar Ni(1)−N(1), Ni(1)−N(2), and average Ni(1)−N(3)/Ni(1)−N(4) distances. The average Ni−O(carboxylate) distance in **3**, **4·CH_2Cl_2**, and **5·1.5CH_2Cl_2** is also similar (~2.10 Å). The carboxylate ligand in each cation is positioned between the phenyl substituents of the 6-Ph_2TPA ligand in a sandwich type motif.

In d_3-acetonitrile, **4·0.5CH_2Cl_2** and **5** (Figure 3) exhibit ^{1}H NMR spectral features that are generally similar to those exhibited by **3** (Figure 1a), including a set of broad resonances in the range 30−50 ppm. These resonances are assigned as β/β'-H's of the pyridyl and phenyl-appended pyridyl rings (inset, Figure 1).[13,16] Relatively sharp resonances

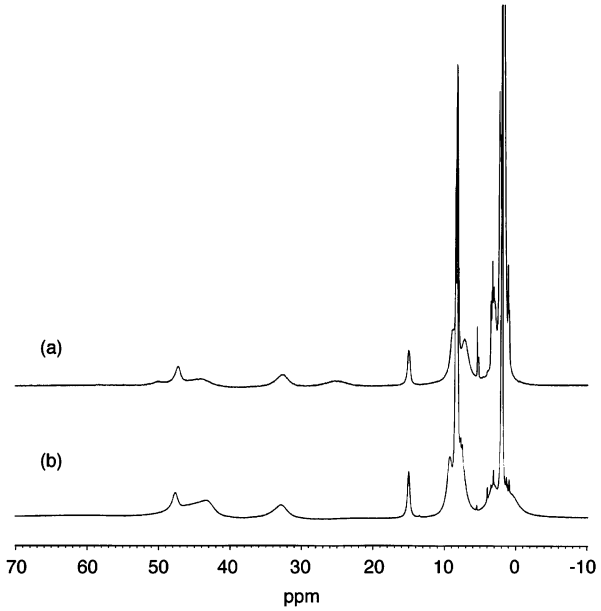

Figure 3. ^{1}H NMR spectra of (a) [(6-Ph_2TPA)Ni($O_2C(CH_2)_2SCH_3$)]ClO_4 (**4·0.5CH_2Cl_2**) and (b) [(6-Ph_2TPA)Ni($O_2CCH_2SCH_3$)]ClO_4 (**5**) in CD_3CN at 25(1) °C.

Table 4. FAB-MS AND UV−vis Spectroscopic Properties of Selected 6-Ph_2TPA-Supported Ni(II) Carboxylate Complexes

	FAB-MS *m/z* $[M - ClO_4]^+$ (100%)	UV−vis [nm] (ϵ, $[M^{-1}\,cm^{-1}]$) (CH_2Cl_2)
3	621	395(39), 562(15), 1047(18)
4·0.5CH_2Cl_2	619	405(25), 570(12), 1050(15)
5	605	400(29), 574(13), 1053(16)
6		395(36), 561(15), 1048(18)
9	545	400(45), 569(31), 1056(38)

at ∼15 ppm in the ^{1}H NMR spectra of **4·0.5CH_2Cl_2** and **5** are assigned as being for the γ-H's in these complexes.

The carboxylate C−O vibrations for **3**, **4·0.5CH_2Cl_2**, and **5** are not easily identifiable in solid-state IR spectra of the complexes due to overlap with vibrations of the 6-Ph_2TPA ligand in the region of 1620−1380 cm^{-1}. Typically, chelating bidentate carboxylate ligands exhibit two vibrations (ν_a and ν_s) with a Δ value (ν_a (CO_2^-) − ν_s(CO_2^-)) less than 200 cm^{-1}.[22] The FAB-MS and UV−vis properties of **3**, **4·0.5CH_2Cl_2**, and **5** are summarized in Table 4.

With the same series of carboxylate ligands as is found in **3**, **4·0.5CH_2Cl_2**, and **5**, in the presence of water, mononuclear 6-Ph_2TPA-ligated Ni(II) complexes having a monodentate carboxylate ligand and one coordinated water molecule have been isolated. These complexes, [(6-Ph_2TPA)Ni(H_2O)(O_2-CPh)]ClO_4 (**6**), [(6-Ph_2TPA)Ni(H_2O)($O_2C(CH_2)_2SCH_3$)]ClO_4 (**7·0.2CH_2Cl_2**), and [(6-Ph_2TPA)Ni(H_2O)($O_2CCH_2SCH_3$)]-ClO_4 (**8**), were characterized by X-ray crystallography, elemental analysis, ^{1}H NMR, and FTIR.

ORTEP representations of the cationic portions of **6·1.75CH_2Cl_2**, **7·0.5CH_2Cl_2**, and **8** are shown in Figure 4. Details of the X-ray data collection and refinement are given in Table 1. Selected bond distances and angles are given in Tables 2 and 3, respectively. A shorter Ni(1)−O(1) interaction (∼2.0 Å) is found in these complexes as compared to

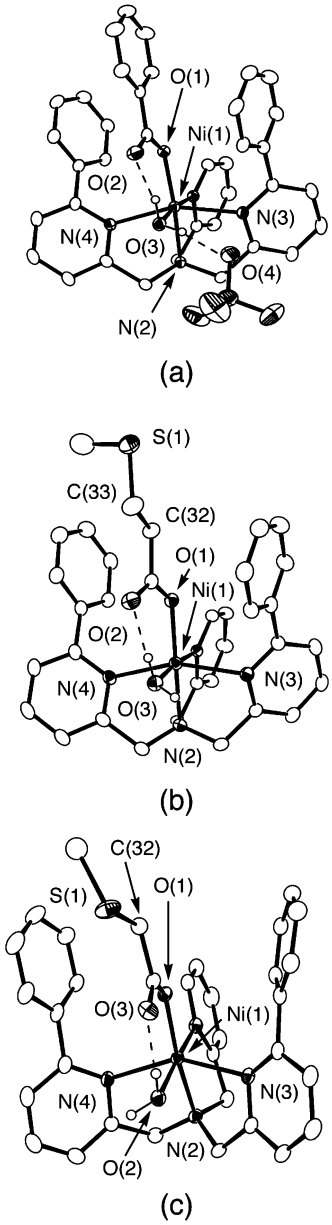

Figure 4. ORTEP representations of (a) **6·1.75CH_2Cl_2**, and the cationic portions of (b) **7·0.5CH_2Cl_2** and (c) **8**. All ellipsoids are drawn at the 35% probability level. Hydrogen atoms other than the water protons omitted for clarity.

the average Ni(1)−O(1) distance (∼2.1 Å) present in the bidentate analogues shown in Figure 2 and previously discussed. The Ni(1)−O(H_2O) distance in this series of complexes ranges from 2.06 to 2.12 Å. A moderately strong hydrogen-bonding interaction is found between a proton of the Ni(II)-bound water molecule and the noncoordinated oxygen atom of the carboxylate ligand.[23] For example, in **6·1.75CH_2Cl_2**, this interaction is characterized by an O(2)···O(3) distance of 2.54 Å and a O(3)−H···O(2) angle of 165°. A summary of the hydrogen-bonding interactions in the cationic portions of **6·1.75CH_2Cl_2**, **7·0.5CH_2Cl_2**, and **8** is given in Table 5.

(22) Nakamoto, K. *Infrared and Raman Spectra of Inorganic and Coordination Complexes*, 5th ed.; Wiley: New York, 1997.

(23) Jeffrey, G. A. *An Introduction to Hydrogen Bonding*; Oxford University Press: New York, 1997.

Table 5. Parameters of Secondary Interactions in 6-Ph_2TPA-Supported Ni(II) Complexes Containing Monodentate Carboxylate Ligands

complex	O(carb)···O(H_2O) (Å)	O(carb)−H···O(H_2O) (deg)	CH···arene centroid (Å)
6·1.75CH_2Cl_2[a]	2.54/2.56	165/165	*b*
7·0.5CH_2Cl_2	2.57	166	3.58/3.57[c]
8	2.62	167	3.65/3.73[d]
9	2.63	164	*b*

[a] Two independent molecules are present in the asymmetric unit of **6·1.75CH_2Cl_2**. [b] Not applicable. [c] The methylene carbon (C(32)), sulfur (S(1)), and methyl carbon (C(33)) atoms of the methylthioacetate ligand exhibit disorder. The CH···arene centroid distances listed are for C(32a)···centroid (C(13)−C(18)) and C(32)···centroid (C(25)−C(30)), respectively. [d] CH···arene centroid distances listed are for C(32)···centroid (C(13)−C(18)) and C(32)···centroid (C(25)−C(30)), respectively.

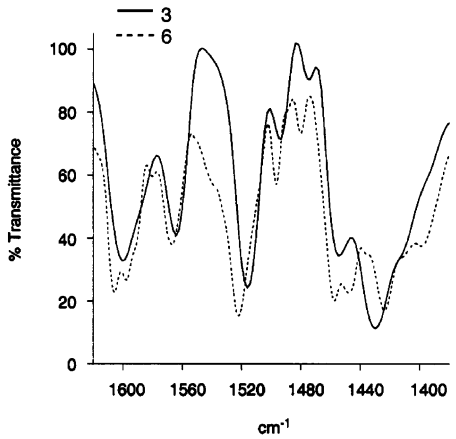

Figure 5. Region of the infrared spectra of **3** and **6**.

Weak CH/π interactions are present between the aliphatic methylene protons of the methylthioalkyl carboxylates in **7·0.5CH_2Cl_2** and **8** and the phenyl appendages of the 6-Ph_2TPA ligand (Table 5).[24] These interactions are indicated by the fact that the distance between an aliphatic carbon (C(32)) of the bound carboxylate and the arene centroid of one or both phenyl groups is less than ~3.7 Å. This distance is the sum of the van der Waals radii of a methyl group and an sp^2 hybridized carbon. Notably, in the bidentate carboxylate derivative **4·0.5CH_2Cl_2** there is only one short CH···centroid distance (3.77 Å, C(32)···arene centroid (C25−C30)), and in **5** there are no CH/π interactions. Therefore, the number of CH/π interactions is higher in complexes having a monodentate methylthioalkyl carboxylate ligand.

In dry acetonitrile, the ^{1}H NMR features of **6**, **7·0.5CH_2Cl_2**, and **8** are identical to those found for the bidentate carboxylate analogues **3**, **4·0.5CH_2Cl_2**, and **5**, respectively, indicating that ^{1}H NMR is not a viable method for determining the carboxylate coordination mode. Comparison of the solid-state (KBr) spectra for the benzoate derivatives **3** and **6** (Figure 5) revealed identifiable differences in the region 1620−1380 cm^{-1}. While the vibrations in this region have not been definitively assigned, the identification of spectroscopic differences does suggest a change in the carboxylate coordination mode.

(24) Nishio, M.; Hirota, M.; Umezawa, Y. *The CH/π Interaction: Evidence, Nature, and Consequences*; Wiley-VCH: New York, 1998.

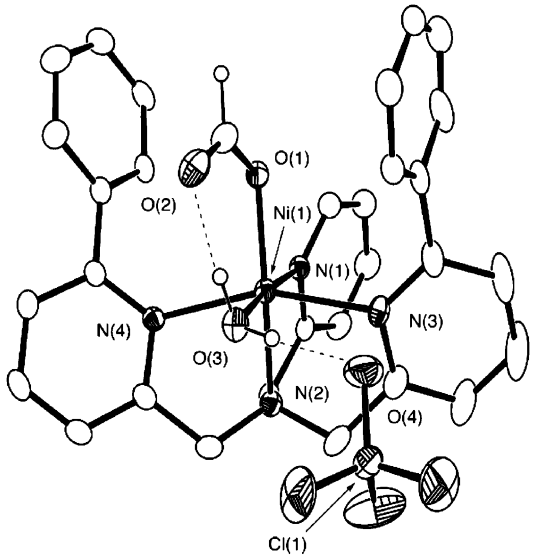

Figure 6. ORTEP representation of [(6-Ph_2TPA)Ni(H_2O)(O_2CH)]ClO_4 (**9**). Ellipsoids are drawn at the 35% probability level. Hydrogen atoms other than the formyl and water protons omitted for clarity.

A 6-Ph_2TPA-Supported Ni(II) Formate Complex. As formic acid is a product of the Ni(II)-ARD-catalyzed reaction shown in Scheme 1, a formate complex (**9**) has been prepared and isolated by combining equimolar amounts of 6-Ph_2TPA, $Ni(ClO_4)_2$·$6H_2O$, and NaO_2CH in methanol/water. We were unable to prepare a water-free Ni(II) formate complex of the 6-Ph_2TPA ligand. This could be due in part to the insolubility of NaO_2CH in dry organic solvents.

An ORTEP representation of **9** is shown in Figure 6. A summary of the data collection and refinement parameters for this structure is given in Table 1. Selected bond distances and angles are given in Tables 2 and 3. The coordination environment of the Ni(II) center in **9** is similar to that found in **6·1.75CH_2Cl_2**, **7·0.5CH_2Cl_2**, and **8**. The Ni(II)-bound water molecule of **9** is involved in two hydrogen-bonding interactions. One of these interactions involves the noncoordinated oxygen atom of the Ni(II)-bound formate. This interaction, which may be classified as a moderate hydrogen-bonding interaction, involves a O(H_2O)···O(formate) heteroatom distance of 2.63 Å (Table 5).[23]

In acetonitrile, **9** exhibits a ^{1}H NMR spectrum with several broad resonances in the 30−50 ppm range (Figure 7). The spectral features are similar to those described above for other monocarboxylate Ni(II) complexes of the 6-Ph_2TPA ligand.[16] A sharp signal at 14.6 ppm is tentatively assigned to the γ hydrogen (see Figure 1 (inset)). Using this signal as a standard integrating to one hydrogen, the signal at 33.7 ppm integrates to two hydrogens and is assigned as a β'-H signal. The overlapping signals in the region 42−50 ppm integrate to a total of four hydrogens and are assigned to the β/β' protons.

The solid-state infrared spectral features of **9** in the region 1620−1380 cm^{-1} are less complicated than those exhibited by **6·1.75CH_2Cl_2**, **7·0.5CH_2Cl_2**, and **8**. However, assignment of the carboxylate C−O vibrations is still not possible due to the presence of vibrations of the 6-Ph_2TPA ligand in the

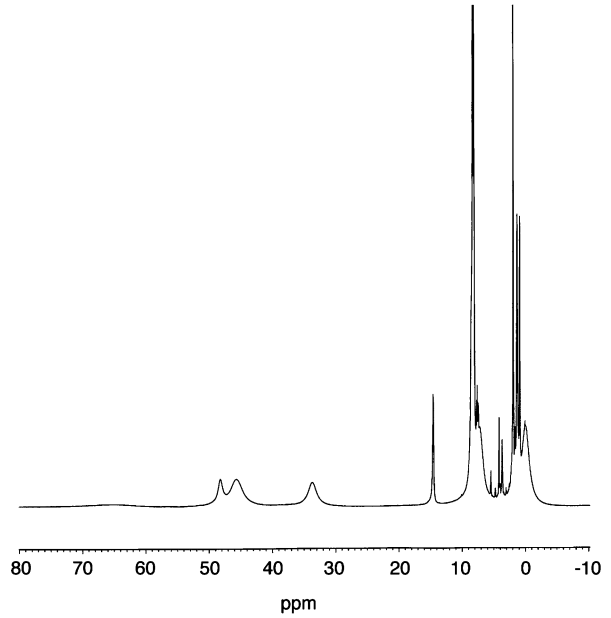

Figure 7. ^{1}H NMR spectrum of [(6-Ph$_2$TPA)Ni(O$_2$CH)(H$_2$O)]ClO$_4$ (**9**) in CD$_3$CN at 25(1) °C.

Table 6. Summary of X-ray Data Collection and Refinement for **10·CH$_3$CN** and **10·CH$_2$Cl$_2$**

	10·CH$_3$CN	**10·CH$_2$Cl$_2$**
empirical formula	$C_{37}H_{48}N_7ClO_6Ni$	$C_{36}H_{47}N_6Cl_3O_6Ni$
fw	780.98	824.86
cryst syst	monoclinic	orthorhombic
space group	$P2_1/n$	$P2_12_12_1$
a (Å)	9.05470(10)	9.1450(2)
b (Å)	16.9928(4)	19.5880(3)
c (Å)	25.0648(6)	21.9762(4)
α (deg)	90	90
β (deg)	93.3772(14)	90
γ (deg)	90	90
V (Å^3)	3849.89(14)	3936.65
Z	4	4
d_{calcd}, Mg m^{-3}	1.347	1.392
temp (K)	150(1)	150(1)
cryst size (mm^3)	0.35 × 0.35 × 0.15	0.33 × 0.15 × 0.08
diffractometer[a]	Nonius Kappa CCD	Nonius Kappa CCD
abs coeff (mm^{-1})	0.627	0.748
2θ max (deg)	54.98	54.98
reflns collected	14094	8749
indep reflns	8675	8749
variable params	659	498
R1/wR2[b]	0.0612/0.1480	0.0581/0.1304
GOF (F^2)	1.066	1.021
largest diff (e Å^{-3})	1.548/−1.406	0.648/−0.591

[a] Radiation used: Mo Kα ($\lambda = 0.71073$ Å). [b] $R1 = \Sigma||F_o| - |F_c||/\Sigma|F_o|$; $wR2 = [\Sigma[w(F_o^2 - F_c^2)^2]/[\Sigma(F_o^2)^2]]^{1/2}$ where $w = 1/[\sigma^2(F_o^2) + (aP)^2 + bP]$.

same region. The mass spectral and UV−vis features of **9** are given in Table 4.

Ni(II) Carboxylate Chemistry in a Hydrogen Bond Donor Secondary Environment. To investigate the influence of the secondary environment on the chemistry of Ni(II) carboxylate species of relevance to acireductone dioxygenase, a series of complexes was prepared using the hydrogen bond donor bnpapa chelate ligand (Scheme 6). Notably, the bidentate benzoate derivative **10** can be isolated under a variety of conditions, including from water-containing solutions. This indicates that, unlike the chemistry of the 6-Ph$_2$TPA-ligated Ni(II) benzoate complexes (**3** and **6**), the presence of water does not induce a shift in the carboxylate coordination mode. Complex **10** has been isolated in two different crystalline forms (**10·CH$_3$CN** and **10·CH$_2$Cl$_2$**). In a dry powdered form, **10** has also been characterized by ^{1}H NMR, FTIR, mass spectrometry, and elemental analysis.

Table 7. Selected Bond Distances and Angles for **10·CH$_3$CN** and **10·CH$_2$Cl$_2$**[a]

	10·CH$_3$CN	**10·CH$_2$Cl$_2$**
Ni(1)−N(2)	2.125(3)	2.124(4)
Ni(1)−N(3)	2.043(3)	2.051(4)
Ni(1)−N(4)	2.136(3)	2.129(3)
Ni(1)−N(6)	2.028(3)	2.021(4)
Ni(1)−O(1)	2.145(3)	2.135(3)
Ni(1)−O(2)	2.099(3)	2.081(3)
O(1)−Ni(1)−O(2)	62.70(10)	62.99(10)
O(1)−Ni(1)−N(2)	92.53(11)	94.68(13)
O(1)−Ni(1)−N(3)	106.75(11)	106.81(13)
O(1)−Ni(1)−N(4)	91.04(11)	89.81(12)
O(1)−Ni(1)−N(6)	167.64(11)	167.70(12)
O(2)−Ni(1)−N(2)	100.24(10)	99.71(12)
O(2)−Ni(1)−N(3)	169.24(11)	169.77(13)
O(2)−Ni(1)−N(4)	97.27(11)	97.94(12)
O(2)−Ni(1)−N(6)	105.04(11)	104.73(13)
N(2)−Ni(1)−N(3)	81.67(12)	81.34(14)
N(2)−Ni(1)−N(4)	161.78(12)	161.91(13)
N(2)−Ni(1)−N(6)	88.06(12)	87.89(14)
N(3)−Ni(1)−N(6)	85.56(12)	85.46(14)
N(4)−Ni(1)−N(6)	92.24(12)	91.43(14)

[a] Estimated standard deviations in the last significant figure are given in parentheses.

Details of the X-ray data collection and refinement for **10·CH$_3$CN** and **10·CH$_2$Cl$_2$** are given in Table 6. Selected bond distances and angles are given in Table 7. An ORTEP representation of the cationic component of **10·CH$_2$Cl$_2$** is shown in Figure 8. The Ni(II) center in both crystalline forms is six-coordinate with the benzoate ligand bound in a bidentate fashion. In **10·CH$_3$CN** the Ni(1)−O(2) bond is ∼0.14 Å shorter than the Ni(1)−O(1) bond. This is interesting as the O(2) atom also acts as a hydrogen bond acceptor for the two secondary amine moieties involving the supporting chelate ligand. Typically, involvement of a metal-bound atom in a hydrogen-bonding interaction results in elongation of the metal−atom bond.[25] In the cationic portion of **10·CH$_2$Cl$_2$**, the difference in bond lengths of the Ni(1)−O(1) and Ni(2)−O(2) bonds is smaller (∼0.05 Å). The Ni(1)−N distances are very similar in **10·CH$_3$CN** and **10·CH$_2$Cl$_2$**. It is important to note that the average Ni(1)−O(carboxylate) bond length in **3**, **10·CH$_3$CN**, and **10·CH$_2$Cl$_2$** all fall in the range 2.08−2.11 Å. Thus, the change in secondary environment from hydrophobic in **3** to a hydrogen bond donor environment in **10·CH$_3$CN** and **10·CH$_2$Cl$_2$** does not produce a notable change in the nickel/carboxylate or nickel/chelate ligand bond distances.

The hydrogen-bonding interactions in **10·CH$_3$CN** and **10·CH$_2$Cl$_2$** involving the secondary amine appendages and one oxygen atom of the bound carboxylate can be described as moderate hydrogen bonds, with heteroatom N···O distances of ∼2.9−3.0 Å.[23] It is noteworthy that this heteroatom

(25) Berreau, L. M. *Eur. J. Inorg. Chem.* **2006**, 273−283.

Scheme 6

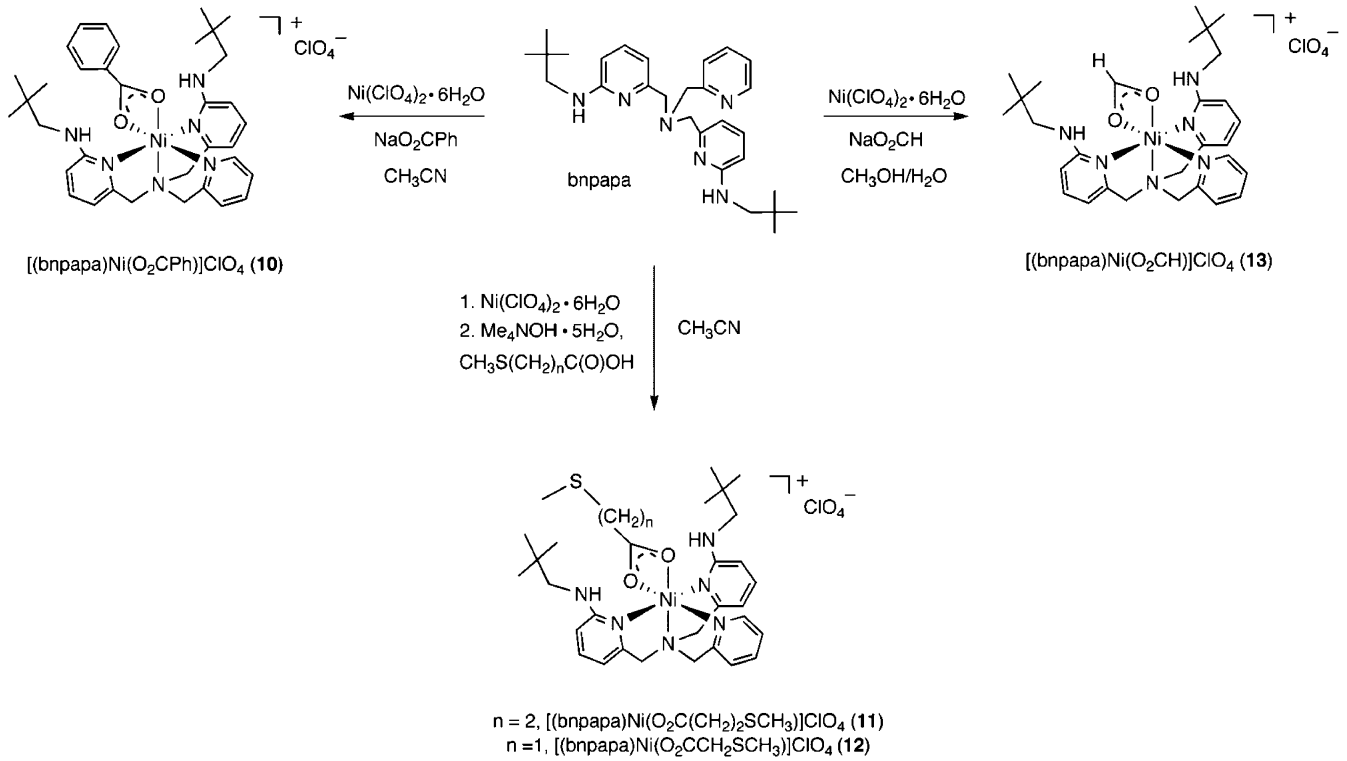

distance is ∼0.3 Å longer than that involving the Ni(II) bound water and carboxylate ligand in **6·1.75CH$_2$Cl$_2$**, **7·0.5CH$_2$Cl$_2$**, **8**, and **9**.

As shown in Scheme 6, two methylthioalkyl carboxylate complexes, [(bnpapa)Ni($O_2C(CH_2)_2CCH_3$)]ClO_4 (**11**) and [(bnpapa)Ni($O_2CCH_2SCH_3$)]ClO_4 (**12**), and a formate complex [(bnpapa)Ni(O_2CH)]ClO_4 (**13**) of the bnpapa ligand, were also prepared and characterized. Complexes **11**−**13** were obtained as microcrystalline solids that were not suitable for X-ray crystallography. However, elemental analysis results confirmed the analytical formulations of these complexes and indicate that no water is present in the isolated crystalline samples.

The ^{1}H NMR features of **10**−**13** are shown in Figure 9. Similar to what is found for 6-Ph$_2$TPA-supported complexes, a series of broad resonances is present in the region 35−70 ppm. Although these have been conclusively assigned, we believe that some of the signals are due to β and β' hydrogens of the pyridyl rings (inset, Figure 9). A signal at ∼15 ppm in the spectrum of each complex (**10**−**13**) is tentatively assigned as the γ proton of the unsubstituted pyridyl ring.

Use of deuterium-labeled derivatives of the bnpapa ligand for the preparation of analogues of **10**−**13** has yielded additional insight into the ^{1}H NMR spectroscopic features of these complexes. The ligands employed, d_6-bnpapa and d_4-bnpapa (Figure 10), contain deuterium atoms at the benzylic or neopentyl methylene positions, respectively. The synthetic procedure used for the preparation of d_6-bnpapa also results in the partial incorporation of deuterium at a β' position. The ^{1}H NMR spectral features of **10-*d*$_6$**, **11-*d*$_6$**, and **13-*d*$_6$** are generally similar to those shown in Figure 9, with a notable decrease in the intensity of a resonance at ∼38−39 ppm relative to the intensity of this resonance in the fully protio parent complexes. Measurement of the ^{2}H NMR spectra of the same series of complexes yielded a relatively sharp signal at ∼38 ppm for each complex. This signal is due to the deuterium incorporation at a β' position in the d_6-bnpapa ligand as noted above. Additionally, in the ^{2}H NMR spectra of **10-*d*$_6$**, **11-*d*$_6$**, and **13-*d*$_6$** a small signal is found at ∼64−65 ppm. This chemical shift matches that of a resonance found in the fully protio parent complexes and suggests minor incorporation of deuterium in the other β' position of the amine-appended pyridyl ring (inset, Figure 9). Resonances for the benzylic $-CH_{2-}$ protons of **10-*d*$_6$**, **11-*d*$_6$**, and **13-*d*$_6$** can be identified only in the ^{2}H NMR spectra. For **10-*d*$_6$**, two broad ^{2}H NMR resonances are found at ∼49 and 25 ppm. These resonances are likely too broad to be observable in the ^{1}H NMR spectrum of the parent complex **10**. On the basis of the symmetry features of the cationic portions of **10·CH$_3$CN** and **10·CH$_2$Cl$_2$**, three benzylic proton resonances are expected.[16] For **10-*d*$_6$**, the third resonance must be too broad to be observable. However, for the methylthiopropionate complex **11-*d*$_6$**, three broad signals are observable at ∼49, 24, and ∼-96 ppm. For the formate derivative **13-*d*$_6$**, only one broad $-CD_{2-}$ feature is identifiable at ∼62 ppm in the ^{2}H NMR spectrum.

Incorporation of deuterium at the neopentyl methylene position in **10-*d*$_4$**, **11-*d*$_4$**, and **13-*d*$_4$** yielded two signals at ∼1.4 and ∼1.1 ppm in the ^{2}H NMR spectrum of each complex. These resonances are not identifiable in the ^{1}H NMR spectrum of the parent **10**, **11**, and **13** complexes due to overlap with the intense *tert*-butyl methyl proton signal at ∼1.5 ppm. The identification of two neopentyl methylene resonances in these complexes is consistent with the "inner"

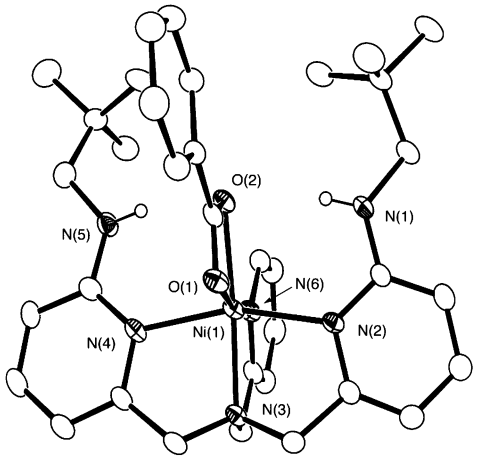

Figure 8. ORTEP representation of the cationic portion of **10·CH$_2$Cl$_2$**. Ellipsoids are drawn at the 35% probability level. Hydrogen atoms other than the secondary amine N−H atoms are omitted for clarity.

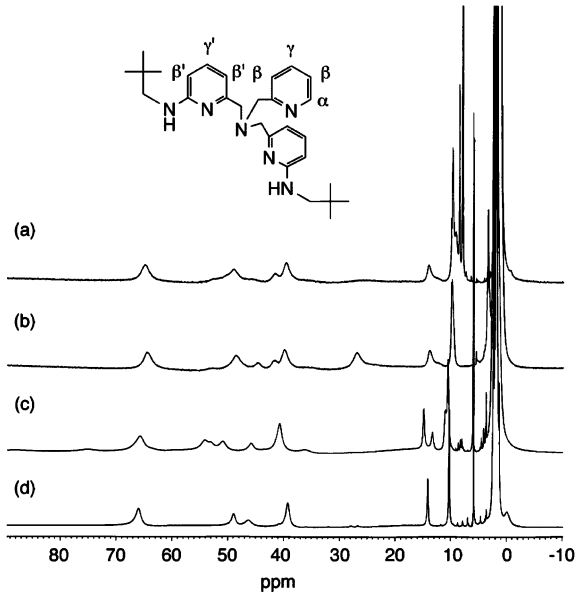

Figure 9. ^{1}H NMR spectra of (a) [(bnpapa)Ni(O$_2$CPh)]ClO$_4$ (**10**), (b) [(bnpapa)Ni(O$_2$C(CH$_2$)$_2$SCH$_3$)]ClO$_4$ (**11**), (c) [(bnpapa)Ni(O$_2$CCH$_2$SCH$_3$)]ClO$_4$ (**12**), and (d) [(bnpapa)Ni(O$_2$CH)]ClO$_4$ (**13**). Spectra were collected at 25(1) °C in CD$_3$CN.

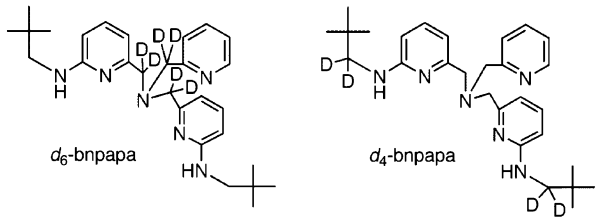

Figure 10. Deuterium-labeled bnpapa ligands: (a) d_6-bnpapa, (b) d_4-bnpapa.

and "outer" chemical environment of these protons in the solid-state structures of **10·CH$_3$CN** and **10·CH$_2$Cl$_2$**.

Addition of D$_2$O to a CD$_3$CN solution of **13** results in the disappearance of a resonance at 48 ppm. We attribute this resonance to being for the secondary amine protons as these are the only easily exchangeable hydrogen atoms in the cationic portion of **13**. The downfield shift of this signal suggests delocalization of unpaired spin density from the Ni(II) center via the hydrogen-bonding interaction involving the metal-bound carboxylate oxygen.

Table 8. Selected Spectroscopic Properties of bnpapa-supported Ni(II) Carboxylate Complexes

	FAB-MS *m*/*z* [M − ClO$_4$]$^+$ (100%)	UV−vis [nm] (ϵ, [M^{-1} cm^{-1}]) (CH$_3$CN)
10	639	556(6), 928(14)
11	637	553(15), 921(22)
12	623	553(19), 921 (22)
13	563	554(18), 884(20)

The solid state (KBr) infrared spectral features of **10**−**13** are similar. There is a broad, intense ν_{N-H} vibration at ∼3300−3350 cm^{-1}. This vibration is found at lower energy and exhibits a stronger intensity than the ν_{N-H} vibration for the free bnpapa ligand, which is consistent with the involvement of the secondary amine N−H donors in hydrogen-bonding interactions.[23] A solution FTIR spectrum of **10** in wet acetonitrile contains features in the region of 1620−1500 cm^{-1} that are identical to those found in the solid-state infrared spectrum of the complex. On the basis of this data, we suggest that the carboxylate ligand in **10**−**13** is bidentate in both the solid-state and in wet acetonitrile solution.

A summary of the mass spectral and UV−vis features of **10**−**13** is given in Table 8. The energy and molar absorptivity of the UV−vis features of **10**−**13** are consistent with d−d type transitions for a pseudo-octahedral Ni(II) center.

Discussion

The Ni(II)-containing enzyme acireductone dioxygenase (Ni(II)-ARD) catalyzes the oxidation of 1,2-dihydroxy-3-keto-5-(methylthio)pentene using O$_2$ to produce methylthiopropionate, formic acid, and CO. In order to investigate mechanistic details of this type of reaction, a synthetic model complex of relevance to a possible enzyme/substrate adduct in Ni(II)-ARD has been prepared, characterized, and evaluated in terms of O$_2$ reactivity.[12] This complex, [(6-Ph$_2$TPA)Ni(PhC(O)C(OH)C(O)Ph)]ClO$_4$ (**1**), which undergoes a Ni(II)-ARD-type reaction with O$_2$ either in the presence or absence of an extra equivalent of base, is supported by a tetradentate chelate ligand containing two hydrophobic phenyl appendages. Inclusion of these phenyl appendages was done to mimic the possible influence of two hydrophobic phenylalanine residues that are positioned near the active site metal center in Ni(II)-ARD.[10] Reaction of **1** with O$_2$ in the presence of 1 equiv of base results in the formation of a Ni(II) biscarboxylate complex ([(6-Ph$_2$TPA)Ni(H$_2$O)(O$_2$CPh)$_2$] (**2**), Scheme 7) having κ^3-coordination of the 6-Ph$_2$TPA chelate ligand. Treatment of **2** with 1 equiv of NH$_4$ClO$_4$ produces a monocarboxylate species [(6-Ph$_2$TPA)Ni(O$_2$CPh)]ClO$_4$ (**3**) and free benzoic acid. In the presence of water, the benzoate ligand in **3** shifts from bidentate to monodentate, with the latter being stabilized in [(6-Ph$_2$TPA)Ni(H$_2$O)(O$_2$CPh)]ClO$_4$ (**6**) by hydrogen-bonding involving a Ni(II)-bound water molecule. Notably, the carboxylate shift chemistry is also found for 6-Ph$_2$TPA-ligated Ni(II) methylthioalkyl carboxylate complexes. Comparative studies of bnpapa-ligated complexes demonstrated that water-dependent car-

Scheme 7

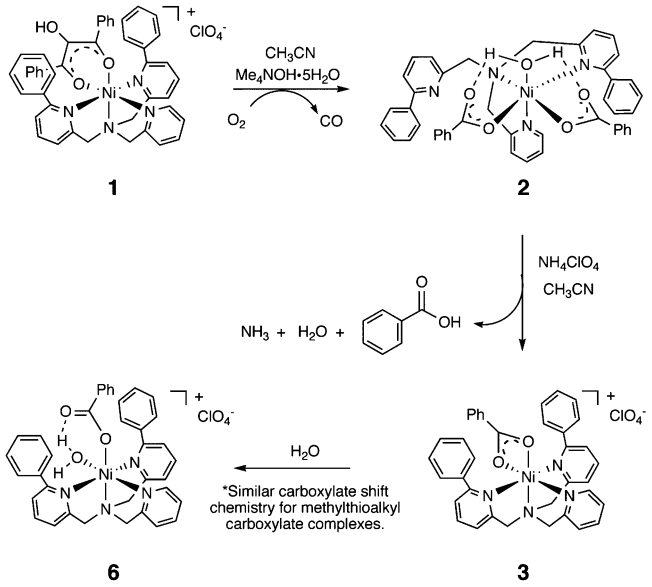

Scheme 8

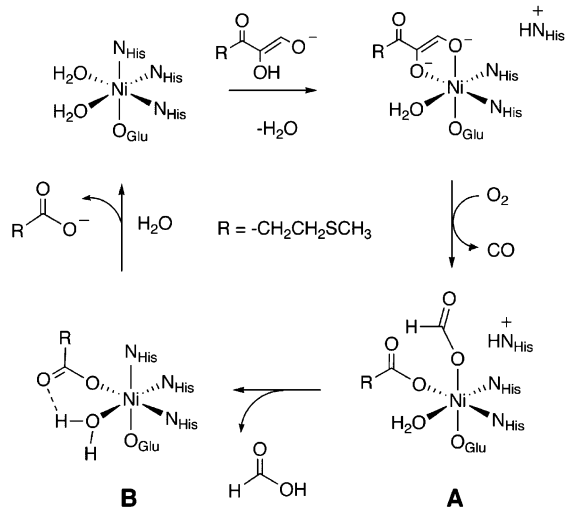

boxylate shift chemistry does not occur in similar complexes having a hydrogen bond donor secondary environment.

The results of the studies presented herein enable the formulation of a possible pathway for stepwise carboxylate product release in Ni(II)-ARD. For the enzyme-catalyzed reaction, release of one carboxylate product from the active site Ni(II) center may be promoted by the protein via a reaction involving a protonated histidine residue. Specifically, EXAFS studies are consistent with the release of a histidine ligand from the Ni(II) center upon coordination of the dianionic form of the substrate (Scheme 8).[9] Following the O_2 reaction, a biscarboxylate Ni(II) species (**A**, Scheme 8) akin to **2** may be formed. The dissociated, protonated histidine residue may provide a proton to promote the release of one caboxylate product (e.g., formate) as the corresponding acid. This reaction has been modeled by treatment of **2** with NH_4ClO_4 to yield **3** and benzoic acid. On the basis of the chemistry found for **6**, **7·0.2CH$_2$Cl$_2$**, **8**, and **9**, in a monocarboxylate Ni(II) species such as **B** (Scheme 8), monodentate carboxylate coordination could be stabilized by a hydrogen-bonding interaction involving a Ni(II)−OH_2 moiety and/or via CH/π interactions involving surrounding aromatic amino acid side chains (e.g., Phe92 and Phe142).[10] This is important, as maintaining a monodentate carboxylate may be key toward ensuring facile release of this ligand. If the carboxylate in the **B** structure (Scheme 8) were instead coordinated bidentate, this may inhibit displacement of this product and reduce the efficiency of the catalytic cycle.[26]

Acknowledgment. We thank the National Institutes of Health (1R15GM072509) for financial support of this work. We thank Thomas Pochapsky for helpful discussions and Casey Winger for technical assistance.

Supporting Information Available: X-ray crystallographic (CIF) files for **4·CH$_2$Cl$_2$**, **5·1.5CH$_2$Cl$_2$**, **6·1.75CH$_2$Cl$_2$**, **7·0.5CH$_2$Cl$_2$**, **8**, **9**, **10·CH$_3$CN**, and **10·CH$_2$Cl$_2$**. This material is available free of charge via the Internet at http://pubs.acs.org.

IC061316W

(26) Bergquist, C.; Fillebeen, T.; Morlok, M. M.; Parkin, G. *J. Am. Chem. Soc.* **2003**, *125*, 6189−6199.